Desalination and Water Treatment
www.deswater.com

doi: 10.5004/dwt.2017.21755

100 (2017) 185–192
December

Study on the removal mechanism of Mg^{2+} by ion exchange resin from wet-process phosphoric acid

Yi Qiu, Cong Tang, Zhiye Zhang, Xinlong Wang, Lin Yang*

School of Chemical Engineering, Sichuan University, Chengdu 610065, Sichuan, China, email: yiqiu911@foxmail.com (Y. Qiu), 603276229@qq.com (C. Tang), zhiyezhang@scu.edu.cn (Z.Y. Zhang), wangxl@scu.edu.cn (X.L. Wang), 18980632893@163.com (L. Yang)

Received 11 April 2017; Accepted 5 December 2017

ABSTRACT

The removal of Mg^{2+} from phosphoric acid by one commercially available cationic resin (001X7)732 was investigated. Effects of various parameters on the removal of Mg^{2+} were studied by batch sorption such as temperature, resin dosage, contact time and initial Mg^{2+} concentration. The results demonstrate that equilibrium of ion exchange was established within 20 min, while more than 90% Mg^{2+} was absorbed. The suitability of pseudo-first-order model, pseudo-second-order model and intra-particle diffusion model were also investigated, results show that the pseudo-second-order kinetic model agrees with the experimental data very well and the sorption follows the Langmuir isotherm. The thermodynamic parameters ΔG,ΔH and ΔS were calculated to be –0.82 kJ·mol^{-1}, 4.80 kJ·mol^{-1}, 18.65 J·mol^{-1}·K^{-1} at 30°C, respectively. The analysis results of the FT-IR indicate that the removal of Mg^{2+} was realized through ion exchange reaction with $-SO_3H$. In addition, the removal efficiency of Mg^{2+} in wet-process phosphoric acid reaches up to 86.8%.

Keywords: Ion exchange; Mg^{2+}; Phosphoric acid ;Kinetics; Thermodynamic

1. Introduction

Phosphoric acid is manufactured in a variety of ways, the most commonly used is wet-process, involving decomposition of phosphate rock with either sulfuric acid, hydrochloric acid, or nitric acid [1]. Although the route of sulfuric acid is widely used, it produces a lot of mineral impurities [2,3]. Particularly, the magnesium impurities in phosphoric acid. If the concentration of MgO in phosphoric acid is more than 1.0%, the high content of magnesium in phosphoric acid will have negative effects on the manufacture of phosphoric acid products. The presence of magnesium will increase the viscosity of the solution and reduce the concentration of hydrogen ions in the phosphoric acid while also affecting the performance of the phosphoric acid products [4]. Therefore, in order to ensure the normal production and subsequent application of wet phosphoric acid (WPA), it is necessary to remove the impurity magnesium ions from phosphoric acid.

Previous researchers reported reasonable methods which include chemical precipitation, crystallization, and organic solvent extraction for purifying phosphoric acid. The use of these techniques are limited due to some limitations, such as limited efficacy, high costs of organic solvents, difficulty in recovering all the solvent from both the raffinate and the purified acid, and environmental pollution by some by-products [5,6].

Ion exchange using polymer resins is an effective unit operation and has been successfully used to remove heavy metal ions from wastewater [7–9]. In addition, Ion exchange resin have been also used for the separation of uranium and rare earths from phosphoric acid [10,11]. Literature searches show that few studies have used resin to purify phosphoric acid.

The main purpose of this work is to measure equilibrium and kinetic parameters of a strongly acidic styrene type cation resin for the removal of Mg^{2+} from prepared phosphoric acid. The effects of temperature, resin dosage,

*Corresponding author.

contact time and initial Mg^{2+} concentration on sorption were also investigated to find the optimum conditions for the sorption process. Moreover, the kinetics, isotherms and thermodynamics for the sorption of Mg^{2+} on resin were also studied. Besides, experiments were carried out to evaluate the removal efficiency in wet-process phosphoric acid for providing important theoretical guidance and technical support in the purification of wet-process phosphoric acid.

2. Materials and methods

2.1. Materials

All chemicals were analytical reagent grade. Phosphoric acid solutions were diluted from pure phosphoric acid, and dissolving with magnesium oxide. The following chemicals were employed: magnesium oxide (MgO), sulfuric acid (H_2SO_4), phosphoric acid (H_3PO_4).

This research was performed using the commercially available ion exchange resin (001X7)732 as provided by Kelong Co., Ltd (Sichuan, China), and this resin is classified as a strongly acidic styrene type cation resin with sulfonic acid functional group. Details of ion exchange resins used in this work are given in Table 1. The resin was conditioned with the following procedure: First, the resin was soaked in 20% sulfuric acid to remove the organic and inorganic impurities. Then, washed with deionized water by method of pumping filtration, this process was carried out until the filtrate becomes clear. Finally, the resin was transferred to a beaker and then dried at 80°C for 24 h. After this, the resin was stored in the beaker covered with preservative film until needed.

2.2. Analytical methods

The Fourier transform infrared (FT-IR) spectrum of the resin was obtained as follow: the resin powder and KBr were mixed uniformly and prepared a tablet of the mixture, the mass ratio of KBr to sample was 100. Nicolet 6700 spectrophotometer (USA) within the range of 500–4000 cm^{-1}. The concentration of Mg^{2+} in the solution was determined by inductively coupled plasma optical emission spectrometry (ICP–OES). The measurements were performed using a Perkin Elmer Optima 7000DV. The calibration range was between 0.2 mg/L and 10 mg/L. Samples over the range of the standards were diluted to be within range.

Table 1
Basic physical and chemical properties of (001X7)732 resin

Properties	Index
Type	Strongly acidic cation
Moisture content (%)	45–55
Total exchange capacity/mmol·g^{-1}	≥4.35
Particle size range (0.315–1.25 mm) (%)	≥95
Grinding ball rate (%)	≥90
Functional group	$-SO_3H$

2.3. Batch experiments

The effects of various parameters on the removal efficiency of Mg^{2+} from phosphoric acid solutions to resin were carried out at different conditions respectively. In all experiments 190 mL of phosphoric solution was poured into the batch reactor and kept in a water bath with magnetic stirring with 120 rpm for 40 min to equilibrium.

In order to reduce the temperature impact, the phosphoric acid solution and resin were preheated to the predetermined temperature before experiment. Aqueous phase was added to the resin. Samples were withdrawn from the solutions at regular intervals of time with 1 g at each size. 13 samples were taken in each experiment but the system was treated as being at constant mass in evaluating results as there is no significant change in mass. Each experiment was carried out three times and the average values were taken as the results.

The calculation of the sorption capacity (q_t, mg/g) and the removal efficiency (E) is given by the mass-balance equation:

$$q_t = \frac{(C_0 - C_t)V}{M} \tag{1}$$

$$E = \frac{C_0 - C_t}{C_0} \times 100\% \tag{2}$$

where C_0 is the initial magnesium concentration in the solution (mg/L), and C_t is the magnesium concentration at time t (mg/L), respectively. V is the volume of solution (L), and M is the resin amount (g).

3. Results and discussions

3.1. Effects of resin dosage

The amount of adsorbent is one of the important factors in the sorption process [12]. The effect of resin dosage on the removal of Mg^{2+} was studied at different dosages (30, 50, 70 and 90 g) by keeping the reaction time at 40 min and initial Mg^{2+} concentration at 9.1 g/L. Fig. 1 shows the sorption process was rapid during the initial minutes and equilibrium was reached after 20 min. The fast sorption rate at the initial stage indicates the presence of freely accessible ion exchange sites on resin surface. Moreover, with the increase of resin dosage, the removal efficiency of Mg^{2+} increases while the amount of Mg^{2+} adsorbed per unit mass of the resin particles decreases. The increase of removal efficiency is due to the increase of the resin dosage resulted in a larger exchangeable area for sorption. However, the observed decrease in the Mg^{2+} uptake per gram of resin particles is possibly due to more un-reacted ion exchange sites was produced during the sorption process when the Mg^{2+} concentration was fixed.

3.2. Effects of temperature on sorption

Effects of reaction temperature on the Mg^{2+} sorption process were investigated in the different reaction temperatures (30, 40, 50, and 60°C) under the sorption time of 40 min. Sorption process can be affected by temperature

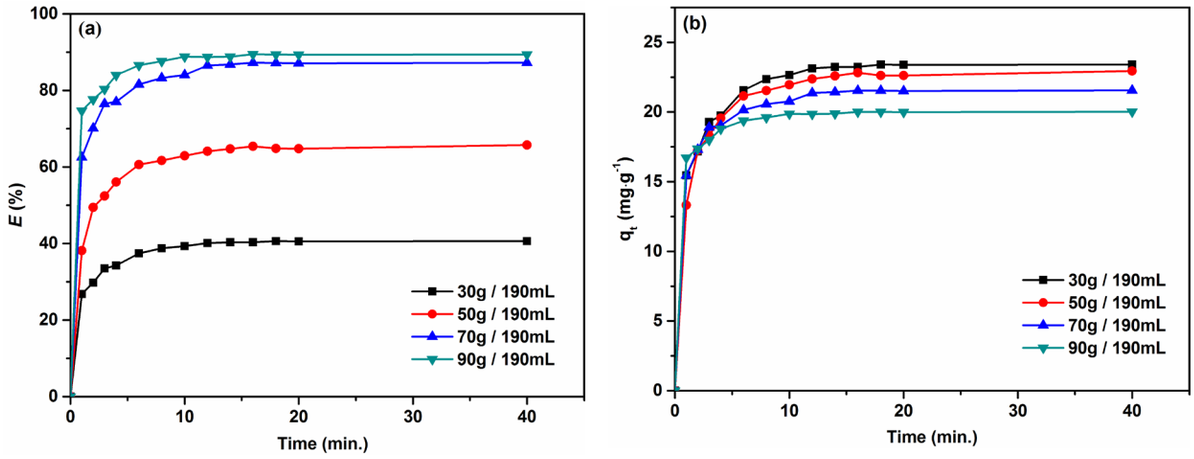

Fig. 1. Effect of resin dosage (a) on magnesium removal from solution (b) on sorption capacity. V = 190 mL, T = 30°C, C_0 = 9.1 g/L.

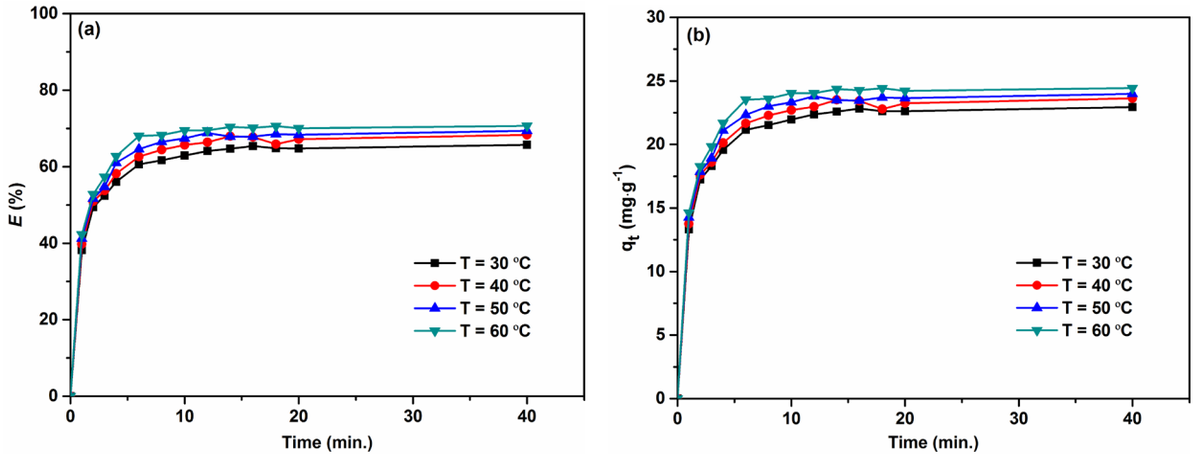

Fig. 2. Effect of temperature (a) on magnesium removal from solution (b) on sorption capacity. V = 190 mL, M = 50 g, C_0 = 9.1 g/L.

in different ways depending on the exothermic or endothermic nature of the process. The results presented in Fig. 2 show the removal efficiency and sorption capacity upon the entire studied temperature range. The removal efficiency increases with increasing temperature, indicating that the sorption process is endothermic process. In addition, a higher sorption capacity at higher temperature can be attributed to the higher diffusion rate of the ions and more active sites due to the expansion of the resin [13].

3.3. Effects of initial Mg^{2+} concentration

To determine the sorption capacity of Mg^{2+}, the effects of initial Mg^{2+} concentration was studied in the range of 4.5–11.3 g/L. As shown in Fig. 3, the equilibrium sorption capacity of Mg^{2+} increases with increase of the initial Mg^{2+} concentration. This is due to higher magnesium concentration can provide greater mass transfer driving force and improve the probability of collisions between magnesium ions and active sites. However, the removal efficiency decrease with the increase of initial Mg^{2+} concentration, which is mainly because of the sorption capacity is fixed for a certain amount of resin.

3.4. Kinetic models

In order to study the mechanism of sorption process, Lagergren's pseudo first-order and Ho's pseudo second-order sorption kinetic models were used to evaluate the behavior of sorption and ion exchange processes.

The pseudo-first-order kinetic model proposed by Lagergren is shown as follows:

$$\frac{dq}{dt} = k_1\left(q_e - q_t\right) \tag{3}$$

where q_t and q_e are the Mg^{2+} concentrations (mg/g) in the solid phases after time t and at equilibrium, respectively, and k_1 (min^{-1}) is the first order rate constant. Integrating Eq. (3) with respect to boundary conditions t = 0 to t = t and

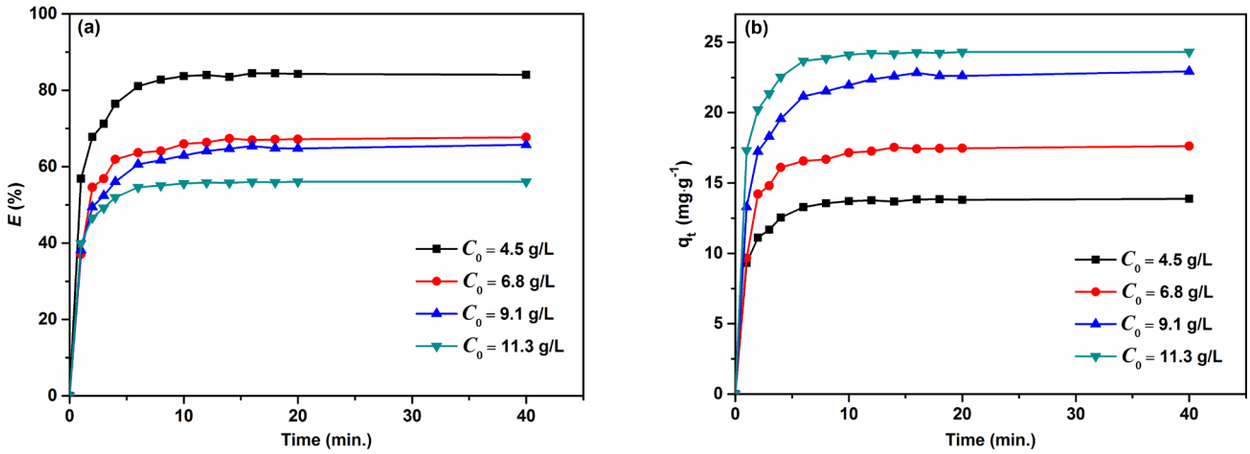

Fig. 3. Effect of initial Mg^{2+} concentration (a) on magnesium removal from solution (b) on sorption capacity. V = 190 mL, M = 50 g, T = 30°C.

Table 2
Parameters for sorption kinetics of Mg^{2+} to resin using different sorption models

C_0/g·L^{-1}	q_e/mg·g^{-1} (exp)	Pseudo-first-order			Pseudo-second-order			Intra-particle diffusion	
		k_1/min^{-1}	q_e/mg·g^{-1}	R^2	k_2/g·mg^{-1}·min^{-1}	q_e/mg·g^{-1}	R^2	k_i/mg·g^{-1}·min$^{1/2}$	R^2
4.5	13.9	0.2658	4.7	0.8906	0.1770	14.1	0.9994	1.0876	0.7420
6.8	17.6	0.2283	6.3	0.8737	0.1135	18.0	0.9991	1.6174	0.6415
9.1	22.9	0.2170	9.7	0.8781	0.0710	23.4	0.9989	2.2646	0.7884
11.3	24.3	0.3597	9.7	0.9294	0.1291	24.7	0.9997	1.6245	0.7090

$q_t = 0$ to $q_t = q_t$, Eq. (4) are obtained. The integrated form is expressed as [14]:

$$\ln\left(q_e - q_t\right) = \ln\left(q_e\right) - k_1 t \tag{4}$$

If the rate of sorption is a second-order mechanism, Ho's [15] pseudo-second-order model can also be used:

$$\frac{dq}{dt} = k_2\left(q_e - q_t\right)^2 \tag{5}$$

Here, k_2 is the second order rate constant (g·mg^{-1}·min^{-1}). By means of integration, this equation can be rearranged as:

$$\frac{t}{q_t} = \frac{1}{k_2 q_e^2} + \frac{t}{q_e} \tag{6}$$

The pore diffusion model is proposed by Weber and Morris [16]. In the intra-particle diffusion model, it is assumed that the sorption capacity varies almost proportionally with $t^{1/2}$ and the model is usually given as [17–19]:

$$q_t = k_i t^{1/2} + C \tag{7}$$

where k_i is the intra-particle diffusion constant (mg·g^{-1}·min$^{1/2}$) and C is the constant.

The relevant values of the parameters and correlation coefficients obtained from the experimental data were shown in Table 2. From the values of R^2, the pseudo-second-order model fits the experimental data best, which indicate that the sorption mechanism is chemisorption.

3.5. Sorption isotherm

3.5.1. Langmuir model

The Langmuir isotherm is a universally applicable model for sorption on a fully homogeneous surface where the interaction between adsorbed molecules can be neglected. The model assumes uniform sorption energies on the surface and the maximum sorption depends on saturation level of monolayer [20]. The Langmuir sorption isotherm can be expressed as [21]:

$$\frac{C_e}{q_e} = \frac{1}{q_m K_L} + \frac{C_e}{q_m} \tag{8}$$

where q_e (mg·g^{-1}) is the amount of Mg^{2+} adsorbed per gram of resin at equilibrium, C_e is the equilibrium concentration of Mg^{2+} in the solution (mg·L^{-1}), q_m (mg·g^{-1}) is the maximum amount of Mg^{2+} per unit weight of resin for complete monolayer coverage and K_L (L·mg^{-1}) is the Langmuir isotherm constant, respectively. The value of q_m and K_L were calculated from the intercept and slope of the plots of C_e/q_e vs. C_e.

3.5.2. Freundlich model

The Freundlich model is known as an empirical equation which is applied for non-ideal and reversible sorption and also can be used for multilayer sorption with non-uniform distribution of sorption affinities and heat over het-

erogeneous surfaces [22]. The linear form of the isotherm is given by the following equation [23]:

$$\ln(q_e)=\frac{1}{n}\ln(C_e)+\ln(K_f) \quad (9)$$

where q_e is the amount of Mg^{2+} adsorbed per gram of resin at equilibrium (mg·g^{-1}), C_e is the equilibrium concentration of Mg^{2+} in the solution (mg·L^{-1}), K_f and n are the Freundlich constants which indicate the sorption capacity and measure of the deviation from linearity, respectively.

The K_f and n (Table 3) parameters were evaluated from the intercept and slope of the linear plots of $\ln(q_e)$ vs. $\ln(C_e)$, respectively. The values of R^2 are higher for Langmuir isotherm which confirms the better applicability of this model.

3.6. Thermodynamics study

The thermodynamic parameters provide in-depth information on energetic changes that are associated with sorption, including the Gibbs free energy ΔG (at equilibrium), the enthalpy change ΔH, and entropy change ΔS (sorption process), which can be estimated by the following equation [24,25]:

$$\Delta G = -RT\ln K_C \quad (10)$$

$$\ln K_C = -\frac{\Delta H}{RT}+\frac{\Delta S}{R} \quad (11)$$

where R is the ideal gas constant [8.314 J·mol^{-1}·K^{-1}], T is the Kelvin temperature. The values of ΔH and ΔS could be obtained as the slope and intercept of the plot between $\ln K_C$ and $1/T$. The equilibrium constant K_C is determined at each temperature using the following equation [26,27]:

$$K_C = \frac{C_{Ae}}{C_e} \quad (12)$$

where C_{Ae} and C_e are the equilibrium concentrations of Mg^{2+} on the adsorbent and in the solution, respectively.

The calculated thermodynamic parameters are shown in Table 4. ΔG values are negative at various temperatures, confirming the sorption is spontaneous. The value of ΔG becomes more negative as temperature increases, indicating the sorption is more effective at higher temperature. The positive values of ΔS suggest an increased randomness at the solid–liquid interface during sorption process [28].

The temperature dependence of most reactions can be determined by the Arrhenius equation [29]:

$$\ln k_2 = \ln A - \frac{E_a}{RT} \quad (13)$$

where k_2 is the pseudo-second-order kinetic equation rate constant, E_a is the activation energy and R and A are the ideal gas constant and Arrhenius factor, respectively.

Plotting $\ln k_2$ vs. 1/T and the slope of the plot gives the E_a/R value, as shown in Fig. 4. The activation energy of the ion exchange reaction is calculated as 32.54 kJ/mol and the temperature has little effect on the exchange reaction, which indicates that the ion exchange is controlled by diffusion. As indicated previously, energy of activation below 50 kJ/mol generally indicated a film and particle diffusion-controlled process, and higher values represented chemical reaction processes [30].

3.7. Characterization of the resin

3.7.1. Analysis of SEM/EDS

Fig. 5 shows the resin before sorption, a relatively large amount of sulfur is detected, which demonstrate the resin is sulfonic type.

Fig. 6 shows the resin after sorption for 30 min at 30°C. The peaks of magnesium are detected after sorption, indicating that magnesium is adsorbed into the resin.

3.7.2. Analysis of FT-IR spectrum

The FT-IR spectrum of before and after sorption are given in Fig. 7. The broad peak around 3,421 cm^{-1} corresponds to the O–H stretching mode. The stretching vibration of C=C bond is observed at peak 1,673 cm^{-1}. The peak observed at 1,400 cm^{-1} indicates the deformation vibration of C–H. The

Table 3
Isotherm constants for Mg^{2+} sorption by (001X7)732 resin

Langmuir			Freundlich		
q_m(mg·g^{-1})	K_L(L·g^{-1})	R^2	K_f(mg·g^{-1})	n	R^2
28.6	0.012	0.96	11.7	1.102	0.91

Table 4
Values of thermodynamic parameters for the sorption process

T/K	ΔG/kJ·mol^{-1}	ΔH/kJ·mol^{-1}	ΔS/J·mol^{-1}·K^{-1}
303	–0.82	4.80	18.65
313	–1.10		
323	–1.23		
333	–1.39		

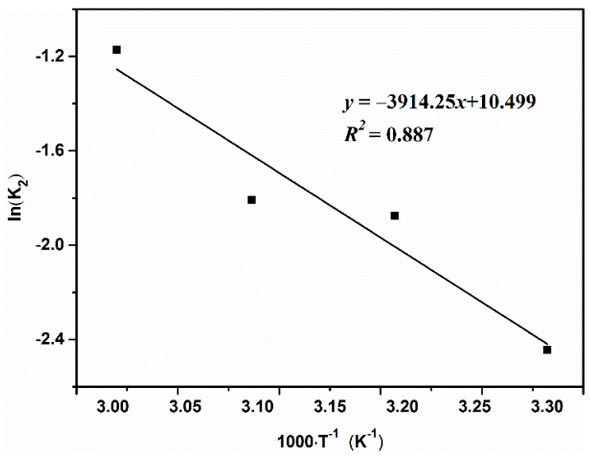

Fig. 4. Plot of ln k_2 against 1/T.

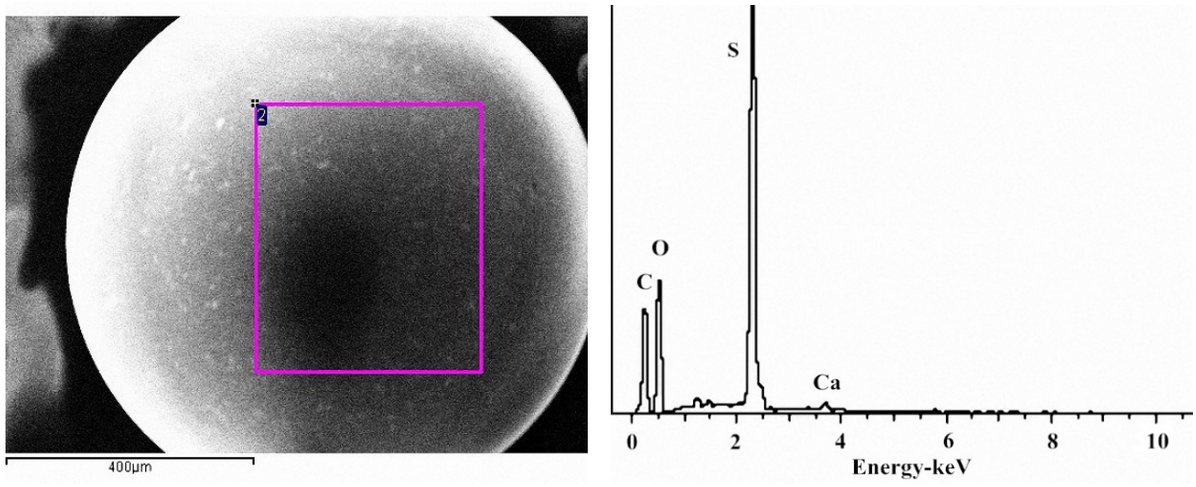

Fig. 5. SEM/EDS pattern of resin before sorption.

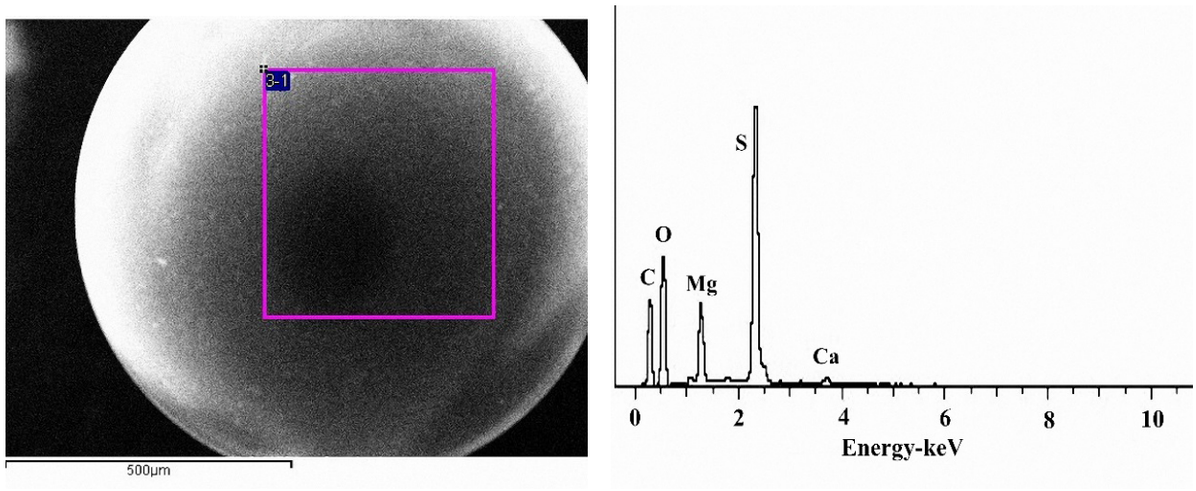

Fig. 6. SEM/EDS pattern of resin after sorption.

founds of three sharp peaks at 1,126 cm^{-1}, 1,037 cm^{-1} and 1,008 cm^{-1} are due to SO_3 symmetric stretching [31]. The peaks at 833 cm^{-1} and 678 cm^{-1} are related to SO. It is also apparent from Fig. 12 that after sorption of Mg^{2+}, the intensity and position of several peaks (3,421 cm^{-1}, 1,037 cm^{-1} and 678 cm^{-1}) had been changed. This indicates that Mg^{2+} was removed though displacement reaction with $–SO_3H$. These results of FT-IR confirm that the resin is a strongly acidic cation resin with sulfonic acid functional group and the Mg^{2+} was removed by resin from phosphoric acid.

3.7.3. Analysis of XPS

The elemental compositions of the ion exchange resin before and after sorption was analyzed by XPS. Fig. 8 shows full-range XPS of the ion exchange resin. There was no significant difference before and after sorption, except for the peak of magnesium after sorption. It can be seen from Fig. 8 that the two predominant peaks at 51.31 eV and 62.57 eV could be assigned to Mg2p and Mg2s [32], which are the typical characteristics of magnesium, indicating that magnesium is adsorbed on the resin. Additionally, the O1s, C1s, S2s, S2p peaks further verify that the resin is sulfonic type, which is in good agreement with the EDS and FTIR results.

3.7.4. Analysis of TG

The thermal behavior of the resin after and before sorption was evaluated by thermogravimetric analysis (TGA) under an air atmosphere. As seen in Fig. 9, the continuous weight losses from room temperature to 340°C and 340°C to 760°C are easy to observe, and the weight has gradually lost as the increasing temperature, with total weight loss of 83.27%. The weight loss before 340°C may be attributed to the interlayer water and volatile materials in the sample. The second stage of weight loss above 340°C should be attributed to the destruction of resin skeleton structure and the decomposition of sulfonic acid functional group [33]. The residual mass of the resin become invariable when

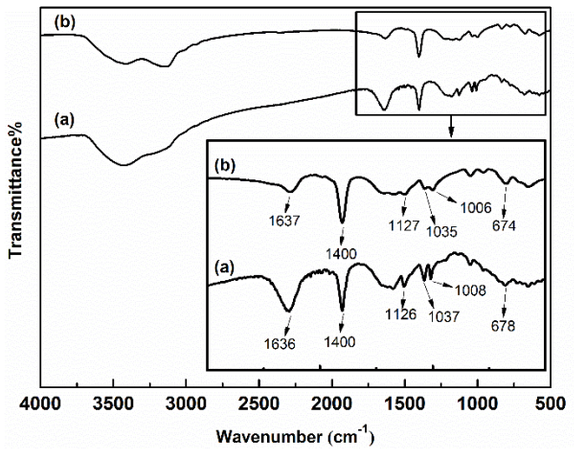

Fig. 7. FT-IR spectrum of resin after (a) and before (b) sorption.

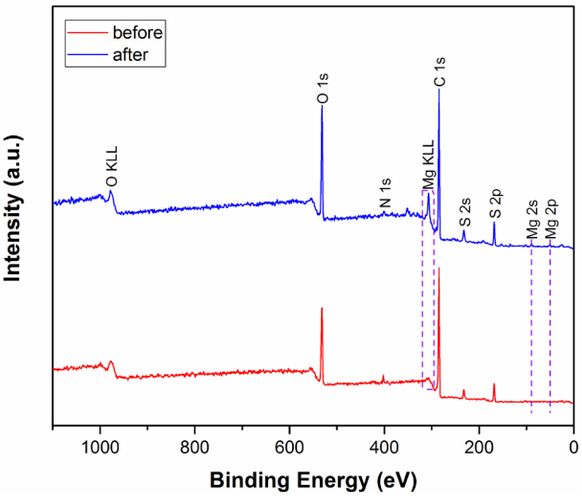

Fig. 8. The XPS spectrum of resin after and before sorption.

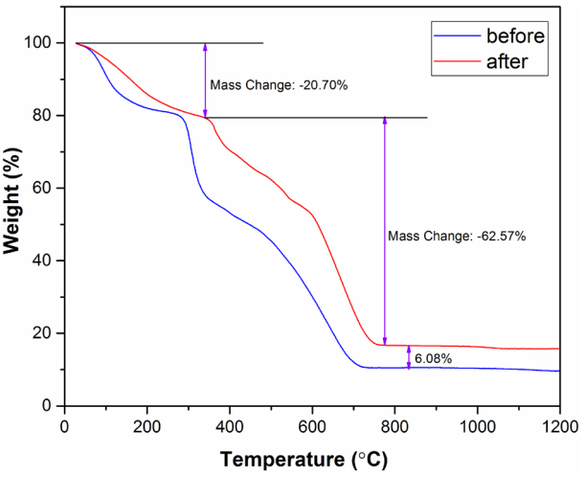

Fig. 9. TGA spectrum of resin after and before sorption. Operative condition: air flow, heating rate 10°C/min.

Table 5
Removal efficiency of metal ions in wet-process phosphoric acid

	P_2O_5%	Mg^{2+}%	Ca^{2+}%
Before	24.75	0.53	0.07
After	24.03	0.07	0.01
Efficiency		86.8	85.7

the temperature increasing to 760°C, indicating the completely decomposed sample and the relevant metal oxides is formed at the same time. The final residue of the resin after sorption is 16.73%, higher than the resin before sorption at 6.08%, it is shown that magnesium does exist in the resin after sorption.

3.8. Removal efficiency of WPA

Experiments were carried out to evaluate the removal efficiency of resin in wet-process phosphoric acid. The phosphoric acid was supported by Yuntianhua Co., Ltd (Yunnan, China). The result presents in Table 5 shows that this resin has a good removal efficiency of Mg^{2+}, the removal efficiency of Mg^{2+} reaches up to 86.8%, and low phosphorus loss. It may be concluded that (001X7)732 resin could be a suitable candidate for the removal of Mg^{2+}in wet-process phosphoric acid.

4. Conclusions

In this study, utilization of a strongly acidic cation-exchange resin for the removal of Mg^{2+} from the phosphoric acid was investigated. The equilibrium of ion exchange is established within 20 min, while more than 90% Mg^{2+} is absorbed. The removal of Mg^{2+} increases with increasing resin dosage, contact time and initial Mg^{2+}concentration, and decreasing with reaction temperature. The kinetics of the process is well described using the pseudo-second-order kinetic equation better than pseudo-first-order kinetic equation. The sorption of Mg^{2+} by resin has a consistency of the Langmuir isotherm, and the maximum sorption capacity was calculated about 28.6 mg/g using Langmuir isotherm model. The activation energy was calculated to be 32.54 kJ/mol. The nature of sorption process is feasible and spontaneous due to negative values of ΔG. In addition, the resin before and after sorption was characterized by means of SEM/EDS, FTIR, XPS and TGA, the results indicate magnesium is adsorbed on the resin. Moreover, the removal efficiency of resin in wet-process phosphoric acid reaches up to 86.8%, and low phosphorus loss. Based on the results of the present work, the (001X7)732 resin could be a suitable candidate for the removal of Mg^{2+} from wet-process phosphoric acid.

Acknowledgment

This work is supported by The National Key Research and Development Program of China (NO.2016YFD0200404).

References

[1] Y. Jin, D. Zou, S. Wu, Y. Cao, J. Li, Extraction kinetics of phosphoric acid from the phosphoric acid—calcium chloride solution by tri-n-butyl phosphate, Ind. Eng. Chem. Res., 54 (2015) 108–116.

[2] A. Bendada, A.H. Meniai, L.M. Bencheikh, Modeling of phosphoric acid purification by liquid-liquid extraction, Chem. Eng. Technol., 24 (2015) 1273–1280.

[3] X. Li, J. Li, Y. Jin, M. Chen, D. Feng, Y. Guo, Wet process of phosphoric acid purification by solvent extraction using tri-n-butyl phosphate and cyclohexanol mixtures, J. Serb. Chem. Soc., 82 (2017) 519–579.

[4] J. Yu, D. Liu, Extraction of magnesium from phosphoric acid using dinonylnaphthalene sulfonic acid, Chem. Eng. Res. Des., 88 (2010) 712–717.

[5] L. Monser, M. Ben Amor, M. Ksibi, Purification of wet phosphoric acid using modified activated carbon, Chem. Eng. Processing: Process Intens., 38 (1999) 267–271.

[6] J. Luo, J. Li, K. Zhou, Y. Jin, Study on Mg^{2+} removal from ammonium dihydrogen phosphate solution by solvent extraction with di-2-ethylhexyl phosphoric acid, Korean J. Chem. Eng., 28 (2011) 1105–1109.

[7] I.H. Lee, Y. Kuan, J. Chern, Factorial experimental design for recovering heavy metals from sludge with ion-exchange resin, J. Hazard. Mater., 138 (2006) 549–559.

[8] N. Öztürk, T.E. Köse, Boron removal from aqueous solutions by ion-exchange resin: Batch studies, Desalination, 227 (2008) 233–240.

[9] T. Guo, S. Wang, X. Ye, H. Liu, X. Gao, Q. Li, M. Guo, Z. Wu, Competitive adsorption of Li, K, Rb, and Cs ions onto three ion-exchange resins, Desal. Water Treat., 51 (2013) 3954–3959.

[10] M. Solgy, M. Taghizadeh, D. Ghoddocynejad, Adsorption of uranium(VI) from sulphate solutions using Amberlite IRA-402 resin: Equilibrium, kinetics and thermodynamics study, Ann. Nucl. Energy, 75 (2015) 132–138.

[11] S. Radhika, V. Nagaraju, B. Nagaphani Kumar, M.L. Kantam, B.R. Reddy, Solid-liquid extraction of Gd(III) and separation possibilities of rare earths from phosphoric acid solutions using Tulsion CH-93 and Tulsion CH-90 resins, J. Rare Earth., 30 (2012) 1270–1275.

[12] M. Naushad, Surfactant assisted nano-composite cation exchanger: development, characterization and applications for the removal of toxic Pb^{2+} from aqueous medium, Chem. Eng. J., 235 (2014) 100–108.

[13] C. Xiong, Y. Li, G. Wang, L. Fang, S. Zhou, C. Yao, Q. Chen, X. Zheng, D. Qi, Y. Fu, Y. Zhu, Selective removal of Hg(II) with polyacrylonitrile-2-amino-1,3,4-thiadiazole chelating resin: Batch and column study, Chem. Eng. J., 259 (2015) 257–265.

[14] Y.S. Ho, G. McKay, Pseudo-second order model for sorption processes, Process Biochem., 34 (1999) 451–465.

[15] Y. Ho, Review of second-order models for adsorption systems, J. Hazard. Mater., 136 (2006) 681–689.

[16] K. Banerjee, G.L. Amy, M. Prevost, S. Nour, M. Jekel, P.M. Gallagher, C.D. Blumenschein, Kinetic and thermodynamic aspects of adsorption of arsenic onto granular ferric hydroxide (GFH), Water Res., 42 (2008) 3371–3378.

[17] S. Rengaraj, C.K. Joo, Y. Kim, J. Yi, Kinetics of removal of chromium from water and electronic process wastewater by ion exchange resins: 1200H, 1500H and IRN97H, J. Hazard. Mater., 102 (2003) 257–275.

[18] N. Dizge, E. Demirbas, M. Kobya, Removal of thiocyanate from aqueous solutions by ion exchange, J. Hazard. Mater., 166 (2009) 1367–1376.

[19] M. Greluk, Z. Hubicki, Sorption of SPADNS azo dye on polystyrene anion exchangers: equilibrium and kinetic studies, J. Hazard. Mater., 172 (2009) 289–297.

[20] B. Alyüz, S. Veli, Kinetics and equilibrium studies for the removal of nickel and zinc from aqueous solutions by ion exchange resins, J. Hazard. Mater., 167 (2009) 482–488.

[21] X. Liu, Y. Li, C. Wang, M. Ji, Cr (VI) Removal by a new type of anion exchange resin DEX-Cr: adsorption affecting factors, isotherms, kinetics, and desorption regeneration, Environ. Prog. Sustain., 34 (2015) 387–393.

[22] A. Arias, I. Saucedo, R. Navarro, V. Gallardo, M. Martinez, E. Guibal, Cadmium(II) recovery from hydrochloric acid solutions using Amberlite XAD-7 impregnated with a tetraalkyl phosphonium ionic liquid, React. Funct. Polym., 71 (2011) 1059–1070.

[23] S. Wei, J. Liu, S. Zhang, X. Chen, Q. Liu, L. Zhu, L. Guo, X. Liu, Stoichiometry, isotherms and kinetics of adsorption of In(III) on Cyanex 923 impregnated HZ830 resin from hydrochloric acid solutions, Hydrometallurgy, 164 (2016) 219–227.

[24] Z. Reddad, C. Gerente, Y. Andres, P. Le Cloirec, Adsorption of several metal ions onto a low-cost biosorbent: kinetic and equilibrium studies, Environ. Sci. Technol., 36 (2002) 2067–2073.

[25] Y. Liu, Y. Liu, Biosorption isotherms, kinetics and thermodynamics, Sep. Purif. Technol., 61 (2008) 229–242.

[26] K. Banerjee, G.L. Amy, M. Prevost, S. Nour, M. Jekel, P.M. Gallagher, C.D. Blumenschein, Kinetic and thermodynamic aspects of adsorption of arsenic onto granular ferric hydroxide (GFH), Water Res., 42 (2008) 3371–3378.

[27] M.R. Yazdani, T. Tuutijärvi, A. Bhatnagar, R. Vahala, Adsorptive removal of arsenic (V) from aqueous phase by feldspars: Kinetics, mechanism, and thermodynamic aspects of adsorption, J. Mol. Liq., 214 (2016) 149–156.

[28] J.N. Israelachvili, Intermolecular and Surface Forces, revised 3rd ed., Academic Press, 2011.

[29] M. Doğan, Y. Özdemir, M. Alkan, Adsorption kinetics and mechanism of cationic methyl violet and methylene blue dyes onto sepiolite, Dyes Pigments, 75 (2007) 701–713.

[30] D.L. Sparks, Kinetics of Soil Chemical Processes, Academic Press, 2013.

[31] P.U. Singare, R.S. Lokhande, R.S. Madyal, Thermal degradation studies of some strongly acidic cation exchange resins, Open J. Phys. Chem., 01 (2011) 45–54.

[32] J. Kwo, G. Wertheim, M. Gurvitch, D. Buchanan, XPS and tunneling study of air-oxidized overlayer structures of Nb with thin Mg, Y and Er, IEEE T. Magn., 19 (2003) 795–798.

[33] C. Xiong, Y. Zheng, Y. Feng, C. Yao, C. Ma, X. Zheng, J. Jiang, Preparation of a novel chloromethylated polystyrene-2-amino-1,3,4-thiadiazole chelating resin and its adsorption properties and mechanism for separation and recovery of Pt(IV) from aqueous solutions, J. Mater. Chem. A, 2 (2014) 5379–5386.